Condensation of $[Ru_3S_2(cymene)_3]^{2+}$ with Sulfide To Give the Dendridic Cluster $[Ru_9S_8(cymene)_6]^{2+}$

Matthew L. Kuhlman and Thomas B. Rauchfuss*

Department of Chemistry, University of Illinois at Urbana-Champaign, Urbana, Illinois 61801

Received May 1, 2004

Summary: Reaction of $[(cymene)_2Ru_3S_2(NCMe)_3]^{2+}$ *with sulfide sources efficiently affords the cluster of clusters* $[(cymene)_6Ru_9S_8](PF_6)_2$*. The synthesis is subject to coformation of* $[(cymene)_4Ru_5S_4](PF_6)_2$*, which arises via the reaction of* $[(cymene)_2Ru_3S_2(NCMe)_3](PF_6)_2$ *and* $[(cymene)_6Ru_9S_8](PF_6)_2$*. Crystallographic analysis demonstrates that* $[(cymene)_6Ru_9S_8](PF_6)_2$ *features three* $[(cymene)_2Ru_3S_2]^{2+}$ *units linked through a pair of* μ_3*-S ligands.*

Introduction

Sulfides derived from $(cymene)Ru^{2+}$ represent an easily accessed family of clusters that display rich redox and ligand substitution.[1,2] We have previously described the photoreactivity of MeCN solutions of $[(cymene)_3Ru_3S_2]^{2+}$, which allows the installation of a variety of donor ligands in place of one labilizable cymene, the intermediate being $[(cymene)_2Ru_3S_2(NCMe)_3]^{2+}$ (Scheme 1).[3,4] In this report, we extend this reaction to include sulfide as the Lewis base.

In the present context, the behavior of $[(cymene)_3Ru_3S_2]^{2+}$ can be described using an analogy between arene ligands and the cluster fragment $(arene)_2Ru_2S_2$, both of which can be considered 6e π-ligands. Thus, $[(arene)_3Ru_3S_2]^{2+}$ can be viewed as the sandwich complex of 12e $[Ru(arene)]^{2+}$ with the metallo ligand η^4-$[(arene)_2Ru_2S_2]$. By extension, this analogy suggests that the *three* cymene ligands in the parent $[(cymene)_3Ru_3S_2]^{2+}$ should be replaceable by $[(arene)_2Ru_2S_2]$ fragments, thereby giving rise to $\{[(arene)_2Ru_2S_2]_3Ru_3S_2\}^{2+}$. A pathway to achieve this cluster condensation is provided by the photolabilization reaction described above (Scheme 1).

Dendridic clusters[5,6] derived via such condensations would be unusual and interesting. Extended Ru−S species in particular are potentially relevant to catalysis, because Ru−S phases are particularly active catalysts for hydrodesulfurization (HDS), more so than typical Mo−Co−S systems currently used industrially.[7,8] Only one Ru−S phase is known: pyrite-like RuS_2.

Scheme 1

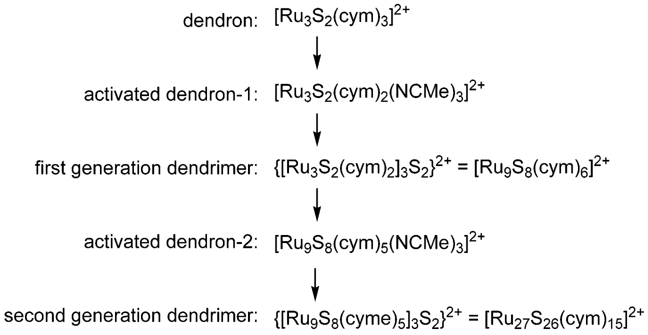

Results and Discussion

$\mathbf{[(cymene)_6Ru_9S_8]^{2+}}$**.** A solution of $[(cymene)_2Ru_3S_2(NCMe)_3]^{2+}$, generated by photolysis of $[(cymene)_3Ru_3S_2]^{2+}$, was found to react with 1.2 equiv of $Na_2S{\cdot}9H_2O$ to produce a 98% yield of $[(cymene)_6Ru_9S_8](PF_6)_2$ ($\mathbf{Ru_9S_8}(PF_6)_2$; Scheme 2). The ^1H NMR spectrum of $\mathbf{Ru_9S_8}^{2+}$ showed that the cymene ligands are equivalent. The formula for $\mathbf{Ru_9S_8}^{2+}$ was also confirmed by ESI-MS with M^{2+} at *m*/*z* 986.3. X-ray crystallographic analysis showed that $\mathbf{Ru_9S_8}^{2+}$ consists of three Ru_3S_2 subclusters sharing a common Ru_3S_2 core (Figure 1). The inner Ru_3S_2 cluster closely resembles that in $[(cymene)_3Ru_3S_2](PF_6)_2$ with regard to the Ru−Ru and Ru−S bond lengths of 2.78 and 2.29 Å, respectively. The three outer Ru_3S_2 clusters are similar to each other but differ from the inner core, with Ru−Ru bonds averaging 2.74 Å. In $[(cymene)_4Ru_5S_4](PF_6)_2$ ($[\mathbf{Ru_5S_4}](PF_6)_2$) the Ru_3 planes are related by 54.8° vs the angles of 55.8° for $\mathbf{Ru_9S_8}^{2+}$, suggesting a common electronic effect.

Extended photolysis of solutions of $\mathbf{Ru_9S_8}^{2+}$ in the presence of $Na_2S{\cdot}9H_2O$ resulted in no further condensation to higher nuclearity Ru/S clusters; the photolysis solutions remained homogeneous, and free cymene was not observed. Solutions of $\mathbf{Ru_9S_8}^{2+}$ slowly decompose to give some $\mathbf{Ru_5S_4}^{2+}$ (see below).

$\mathbf{[(cymene)_4Ru_5S_4]^{2+}}$**.** With fewer equivalents of sulfide, the main product is $\mathbf{Ru_5S_4}^{2+}$, which had been previously isolated in trace amounts from the prolonged photolysis of $\mathbf{Ru_3S_2}^{2+}$.[3] The use of NaSH often leads to cleaner syntheses (55% yield). The formation of $\mathbf{Ru_5S_4}^{2+}$ appears to proceed via the initial formation of $\mathbf{Ru_9S_8}^{2+}$,

---

* To whom correspondence should be addressed. E-mail: rauchfuz@uiuc.edu.

(1) Lockemeyer, J. R.; Rauchfuss, T. B.; Rheingold, A. L. *J. Am. Chem. Soc.* **1989**, *111*, 5733.

(2) Seino, H.; Mizobe, Y.; Hidai, M. *New J. Chem.* **2000**, *24*, 907−911.

(3) Eckermann, A. L.; Fenske, D.; Rauchfuss, T. B. *Inorg. Chem.* **2001**, *40*, 1459−1465.

(4) Kuhlman, M. L.; Rauchfuss, T. B. *Inorg. Chem.* **2004**, *43*, 430−435.

(5) Albinati, A.; Leoni, P.; Marchetti, L.; Rizzato, S. *Angew. Chem., Int. Ed.* **2003**, *42*, 5990−5993. Mas-Ballesté, R.; Clegg, W.; Lledós, A.; González-Duarte, P. *Eur. J. Inorg. Chem.* **2004**, 3223−3227.

(6) Roland, B. K.; Carter, C.; Zheng, Z. *J. Am. Chem. Soc.* **2002**, *124*, 6234−6235.

(7) Cai, T.; Song, Z.; Rodriguez, J. A.; Hrbek, J. *J. Am. Chem. Soc.* **2004**, *126*, 8886−8887.

(8) Chianelli, R. R.; Berhault, G.; Raybaud, P.; Kasztelan, S.; Hafner, J.; Toulhoat, H. *Appl. Catal., A* **2002**, *227*, 83−96.

10.1021/om0496941 CCC: $27.50

Scheme 2

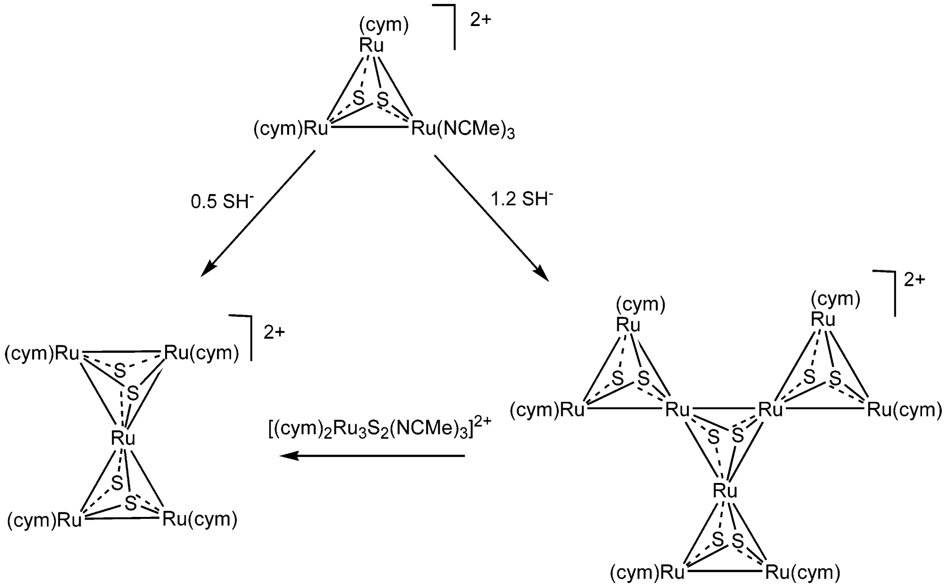

which is attacked by the unreacted [(cymene)$_2$Ru$_3$S$_2$(NCMe)$_3$]$^{2+}$. Consistent with this hypothesis, addition of 2 equiv of [(cymene)$_2$Ru$_3$S$_2$(NCMe)$_3$]$^{2+}$ to **Ru$_9$S$_8$**$^{2+}$ resulted in a nearly quantitative conversion to **Ru$_5$S$_4$**$^{2+}$ (90%). To prevent the formation of **Ru$_5$S$_4$**$^{2+}$ excess Na$_2$S·9H$_2$O (1.2 equiv) is needed—if the exact stoichiometry (0.66 equiv) of Na$_2$S·9H$_2$O is added, a substantial amount of **Ru$_5$S$_4$**$^{2+}$ (40%) is formed with **Ru$_9$S$_8$**$^{2+}$.

In an attempt to probe the cluster condensation pathway, we treated [(cymene)$_2$Ru$_3$S$_2$(NCMe)$_3$]$^{2+}$ with varying amounts of PPh$_4$TeH.[9] ESI-MS analysis showed that these reactions produced mainly **Ru$_5$S$_4$**$^{2+}$, not Te-containing products such as **Ru$_5$S$_{4-x}$Te$_x$**$^{2+}$. With 1.1 equiv of PPh$_4$TeH, a species of unknown structure, [Ru$_6$(cymene)$_4$S$_2$Te$_2$]$^{2+}$ (*m*/*z* 763), was a major product, as indicated by ESI-MS.

Summary

The present work extends the range of ligands that react with [(cymene)$_2$Ru$_3$S$_2$(NCMe)$_3$]$^{2+}$. The condensation reactions are proposed to proceed via the sulfido-bridged dimer of clusters [(cymene)$_2$S$_2$Ru$_3$S$_2$Ru$_3$S$_2$(cymene)$_2$] or MeCN adducts thereof. Related unsaturated sulfido and thiolato species include Cp*$_2$Rh$_2$S$_2$ and (C$_6$Me$_6$)Ru(SAr)$_2$.[10,11] Ru$_3$S$_2$Ru$_3$ species with a square Ru$_2$S$_2$ core would be suited for condensation with [(cymene)$_2$Ru$_3$S$_2$(NCMe)$_3$]$^{2+}$, yielding **Ru$_9$S$_8$**$^{2+}$. We were unable to convert **Ru$_9$S$_8$**$^{2+}$ or **Ru$_5$S$_4$**$^{2+}$ into larger clusters because their arene ligands are nonlabile. The effect of different arene ligands merits further investigation.

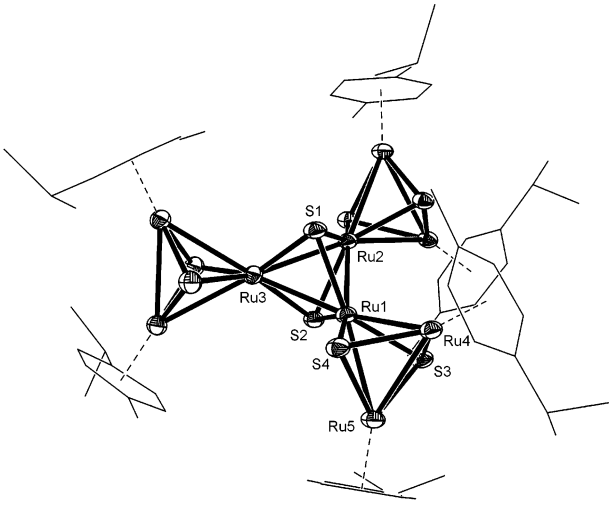

Figure 1. Molecular structure of [(cymene)$_6$Ru$_9$S$_8$](PF$_6$)$_2$ showing the atom-labeling scheme. Thermal ellipsoids are drawn at the 50% level.

Materials and Methods

General Considerations. Standard Schlenk techniques were used in all syntheses. An immersion reactor (150 mL) with a water-cooled quartz sheath was used for photolysis. The UV light source was a medium-pressure mercury-vapor lamp (Hanovia, 200 W). ^{1}H NMR spectra were acquired on Unity Varian 400 and 500 spectrometers. Elemental analyses were determined by the Microanalytical Laboratory at the School of Chemical Sciences.

[(cymene)$_6$Ru$_9$S$_8$](PF$_6$)$_2$ ([Ru$_9$S$_8$](PF$_6$)$_2$). A solution of 628 mg (0.592 mmol) of [(cymene)$_3$Ru$_3$S$_2$](PF$_6$)$_2$ in 60 mL of MeCN was photolyzed for 1 h before being treated dropwise with a solution of 176 mg (0.733 mmol) of Na$_2$S·9H$_2$O (Aldrich) in 15 mL of H$_2$O. After 1 h, the resulting black solution was evaporated to dryness. The solid was extracted into 40 mL of CH$_2$Cl$_2$, which was also evaporated to leave a solid. The product was re-extracted into 10 mL of THF and reprecipitated with 120 mL of hexane. Yield: 439 mg (98%). ^{1}H NMR (MeCN): 1.27 (d, 6H), 2.22 (s, 3H), 2.56 (sept, 1H), 5.47 (q, 4H). ESI-MS: *m*/*z* 986.6 ([M^{2+}]). Anal. Calcd (found) for C$_{60}$H$_{84}$F$_{12}$P$_2$Ru$_9$S$_8$: C, 31.87 (31.73); H, 3.74 (4.01); N, 0 (0.19). Crystals for X-ray diffraction grew over the course of 2 weeks by vapor diffusion of Et$_2$O into a solution of 25 mg of **[Ru$_9$S$_8$]**(PF$_6$)$_2$ in 3 mL of MeCN.

[(cymene)$_4$Ru$_5$S$_4$](PF$_6$)$_2$ ([Ru$_5$S$_4$](PF$_6$)$_2$). A solution of 213 mg (0.201 mmol) of [(cymene)$_3$Ru$_3$S$_2$](PF$_6$)$_2$[1] in 45 mL of MeCN was irradiated with UV light with stirring for 1 h. The resulting solution was treated dropwise with a solution of 6

---

(9) Houser, E. J.; Rauchfuss, T. B.; Wilson, S. R. *Inorg. Chem.* **1993**, *32*, 4069−76.

(10) Dobbs, D. A.; Bergman, R. G. *Inorg. Chem.* **1994**, *33*, 5329−5336.

(11) Mashima, K.; Mikami, A.; Nakamura, A. *Chem. Lett.* **1992**, 1473−1476.

Table 1. Crystallographic Data for $[(cymene)_6Ru_9S_8](PF_6)_2$

empirical formula	$C_{60}H_{84}F_{12}P_2Ru_9S_8$
fw	2261.41
space group	$P\bar{1}$
cryst size (mm^3)	0.42 × 0.32 × 0.28
temp (K)	193(2)
λ (Å)	0.710 73
a (Å)	15.076(5)
b (Å)	17.410(5)
c (Å)	32.621(10)
α (deg)	88.052(5)
β (deg)	86.399(5)
γ (deg)	66.131(5)
V (Å^3)	11 039(5)
Z	4
ρ_{calcd} (Mg/m^3)	1.957
μ(Mo Kα) (mm^{-1})	2.009
min/max transmissn	0.3905/0.6697
no. of measd/indep rflns	81 449/28 611
no. of data/restraints/params	28 611/5155/2186
F(000)	4512
GOF	1.057
R_{int}	0.0649
R1 ($I > 2\sigma$) (all data)[a]	0.0540 (0.0963)
wR2 ($I > 2\sigma$) (all data)[b]	0.1133 (0.1271)
max peak/hole (e/Å^3)	1.550/−1.240

[a] $R1 = \sum||F_o| - |F_c||/\sum|F_o|$. [b] $wR2 = \{\sum[w(F_o^2 - F_c^2)^2]/\sum[w(F_o^2)^2]\}^{1/2}$.

mg (0.107 mmol) of NaSH in 5 mL of H_2O. The reaction solution was evaporated to dryness, and the solid residue was rinsed with 3 mL of THF and 10 mL of H_2O. The product was extracted into ca. 5 mL of acetone and reprecipitated with 80 mL of Et_2O to give a red-brown powder, which was filtered and washed with Et_2O. Yield: 84 mg (55%). ^1H NMR (MeCN): 1.27 (d, 6H), 2.23 (s, 3H), 2.55 (sept, 1H), 5.65 (q, 4H). ESI-MS: m/z 585 ([M^{2+}]). These data match those previously reported.[3]

Crystallography. Crystals were mounted on thin glass fibers using Paratone-N oil (Exxon) before being transferred to a Siemens Platform/CCD automated diffractometer for data collection. Data processing was performed with SAINT PLUS, version 6.22. Structures were solved using direct methods and refined using full-matrix least squares on F^2 using the Bruker program SHELXTL, version 6.10. Hydrogen atoms were fixed in idealized positions with thermal parameters 1.5 times those of the attached carbon atoms. The data were corrected for absorption on the basis of ψ scans. Specific details for each crystal are given in Table 1; selected bond distances and angles are given in Table 2. Full crystallographic details have been deposited with the Cambridge Crystallographic Data Center as Supplementary Publication No. CCDC-239367.

Table 2. Selected Bond Distances (Å) and Angles (deg) for $[(cymene)_6Ru_9S_8](PF_6)_2$

Ru(1)−Ru(2)	2.788(1)	Ru(4)−S(4)	2.299(2)
Ru(1)−Ru(4)	2.804(1)	Ru(1)−S(1)	2.274(2)
Ru(4)−Ru(5)	2.714(1)	Ru(1)−S(4)	2.256(2)

Ru(4)−Ru(1)−Ru(5)	57.35(3)	S(1)−Ru(1)−S(2)	91.39(8)
Ru(3)−Ru(1)−Ru(2)	59.74(3)	S(4)−Ru(5)−S(3)	89.51(9)
Ru(1)−Ru(5)−Ru(4)	60.45(3)	S(1)−Ru(1)−S(4)	107.57(8)

Acknowledgment. This research was supported by the NSF. We thank Scott Wilson and Teresa Prussak-Wieckowska for assistance with the X-ray crystallography.

Supporting Information Available: Crystallographic data (CIF format), including experimental details and complete tables of bond distances and angles, atomic coordinates, and anisotropic displacement parameters. This material is available free of charge via the Internet at http://pubs.acs.org.

OM0496941